Synthesis and Initial Evaluation of YM-08, a Blood-Brain Barrier Permeable Derivative of the Heat Shock Protein 70 (Hsp70) Inhibitor MKT-077, Which Reduces Tau Levels

Yoshinari Miyata,[†] Xiaokai Li,[†] Hsiu-Fang Lee,[‖] Umesh K. Jinwal,[⊥] Sharan R. Srinivasan,[†] Sandlin P. Seguin,[#] Zapporah T. Young,[†] Jeffrey L. Brodsky,[#] Chad A. Dickey,[⊥] Duxin Sun,[‖] and Jason E. Gestwicki*,[†,‡,§]

[†]Life Sciences Institute and the Departments of [‡]Pathology, [§]Biological Chemistry, and [‖]Pharmaceutical Sciences, University of Michigan, Ann Arbor, Michigan, United States
[⊥]Department of Molecular Medicine, University of South Florida, Tampa, Florida, United States
[#]Department of Biological Sciences, University of Pittsburgh, Pittsburgh, Pennsylvania, United States
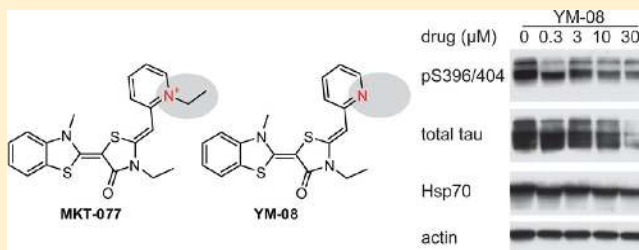
Ⓢ Supporting Information

ABSTRACT: The molecular chaperone, heat shock protein 70 (Hsp70), is an emerging drug target for treating neurodegenerative tauopathies. We recently found that one promising Hsp70 inhibitor, MKT-077, reduces tau levels in cellular models. However, MKT-077 does not penetrate the blood-brain barrier (BBB), limiting its use as either a clinical candidate or probe for exploring Hsp70 as a drug target in the central nervous system (CNS). We hypothesized that replacing the cationic pyridinium moiety in MKT-077 with a neutral pyridine might improve its clogP and enhance its BBB penetrance. To test this idea, we designed and synthesized YM-08, a neutral analogue of MKT-077. Like the parent compound, YM-08 bound to Hsp70 in vitro and reduced phosphorylated tau levels in cultured brain slices. Pharmacokinetic evaluation in CD1 mice showed that YM-08 crossed the BBB and maintained a brain/plasma (B/P) value of ∼0.25 for at least 18 h. Together, these studies suggest that YM-08 is a promising scaffold for the development of Hsp70 inhibitors suitable for use in the CNS.

KEYWORDS: Allosteric inhibitors, microtubule-associated protein tau (MAPT), Alzheimer's disease, tauopathy, proteostasis, protein quality control, rhodacyanines

Tau is a microtubule-binding protein that aberrantly accumulates in 15 neurodegenerative disorders, including Alzheimer's disease (AD).[1,2] One potential way to treat AD and other tauopathies may be to reduce the levels of tau, especially the hyperphosphorylated and proteolyzed forms that are most prone to aggregation.[3−6]

Tau homeostasis is normally controlled through the action of molecular chaperones, such as heat shock protein 70 (Hsp70).[7−9] Hsp70 prevents accumulation of tau by assisting tau rebinding to microtubules[10] and shuttling excess tau to the ubiquitin-proteasome and autophagy systems for degradation.[7,11] In cellular models, inhibitors of the ATPase activity of Hsp70 have been shown to favor tau turnover and "re-set" its homeostasis.[12] Moreover, first-generation Hsp70 inhibitors, such as methylene blue (MB), improve learning and memory in mouse models of tauopathy,[13,14] suggesting that this strategy holds promise for the eventual treatment of AD and other tauopathies.

One of the challenges facing clinical deployment of this approach is that relatively few Hsp70 inhibitors are known and many of the first generation compounds, such as MB, are not selective for Hsp70.[8,15,16] In fact, only a handful of known Hsp70 inhibitors, including 115-7c[17,18] and MKT-077,[19,20] are Hsp70-selective in cells and none of these compounds are known to pass the blood-brain barrier (BBB). Accordingly, the major objective of this study was to generate an analogue that might be suitable for use in the CNS. We reasoned that a BBB penetrant Hsp70 inhibitor could be used to further probe the relationship between Hsp70 and tau homeostasis in vivo and that such a compound might serve as a lead for the development of anti-tau therapies.
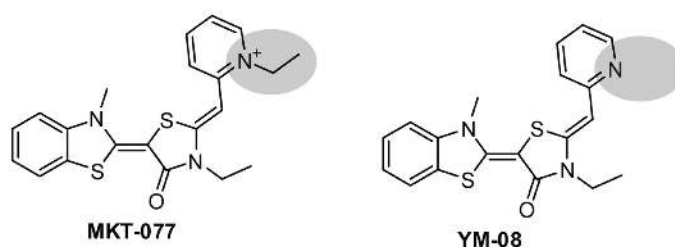
MKT-077 is a delocalized cationic rhodacyanine (Figure 1A) that selectively binds Hsp70 in cells, based on biochemical[19,21,22] and genetic studies.[20,21] Recent NMR studies have shown that MKT-077 binds to an allosteric pocket in the nucleotide-binding domain (NBD) of Hsc70,[23] an abundant, cytoplasmic member of the Hsp70 family. This binding site is highly conserved and

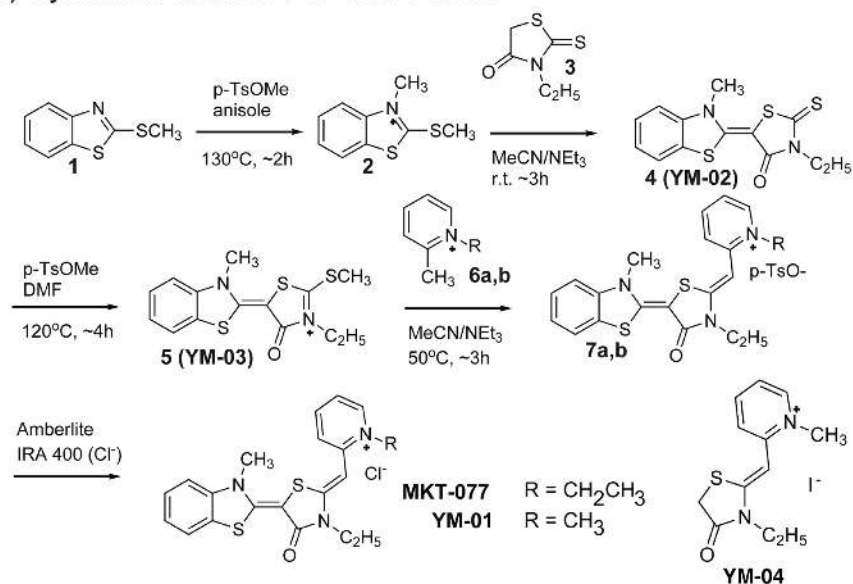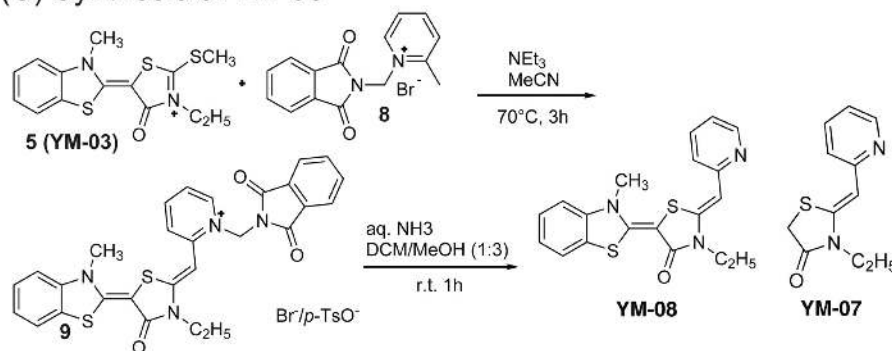**Figure 1.** Synthesis of MKT-077 and its derivatives. (A) Chemical structures of MKT-077 and YM-08, highlighting the pyridine ring. (B) Synthetic route used to generate cationic molecules, MKT-077, YM-01, and the intermediates YM-02 and YM-03. Overall yield of MKT-077 and YM-01 was ~25%. (C) Synthetic route to neutral YM-08, starting from common intermediate 5 (YM-03). Overall yield of YM-08 was ~25%. The structures of two control compounds, YM-04 and YM-07, are shown.

MKT-077 is active against other family members, such as mitochondrial and prokaryotic Hsp70s.[19,21] Pioneering efforts by Chen, Wadhwa, and others have shown that MKT-077 and its analogs bind Hsp70 family members and that they have anti-cancer activity in multiple cancer lines, including melanoma cells and carcinomas of the colon, breast and pancreas.[20,22,24−26] Based on these observations, MKT-077 advanced to a phase I clinical study as an anti-cancer agent; however, progress was halted due to its nephrotoxicity in a subset of patients.[27,28] Renal damage was likely exacerbated by the dramatic accumulation of MKT-077 in the kidney, as shown by whole animal imaging and

pharmacodynamic studies.[29] Moreover, these same studies confirmed that MKT-077 does not cross the BBB,[30] blunting any potential use in treating or studying neurodegenerative diseases. Together, these problems have limited use of MKT-077, especially in CNS disorders.

We hypothesized that the poor brain exposure of MKT-077 might arise, in part, from its cationic pyridinium, which contributes to predicted physicochemical properties (clogP −0.9; tPSA 26.6) that are not typically associated with CNS penetration.[31] Accordingly, we wanted to explore whether replacing this group with a neutral pyridine might be sufficient to improve BBB

(A) YM-08 binds Hsc70 by ELISA

cmpd	IC_{50} (μM) $\pm$ SEM
MKT-077	6.4 $\pm$ 0.23
YM-01	3.2 $\pm$ 0.23
YM-08	0.61 $\pm$ 0.05
YM-02	>50
YM-03	>50
YM-04	15 $\pm$ 3.0
YM-07	5.8 $\pm$ 1.5

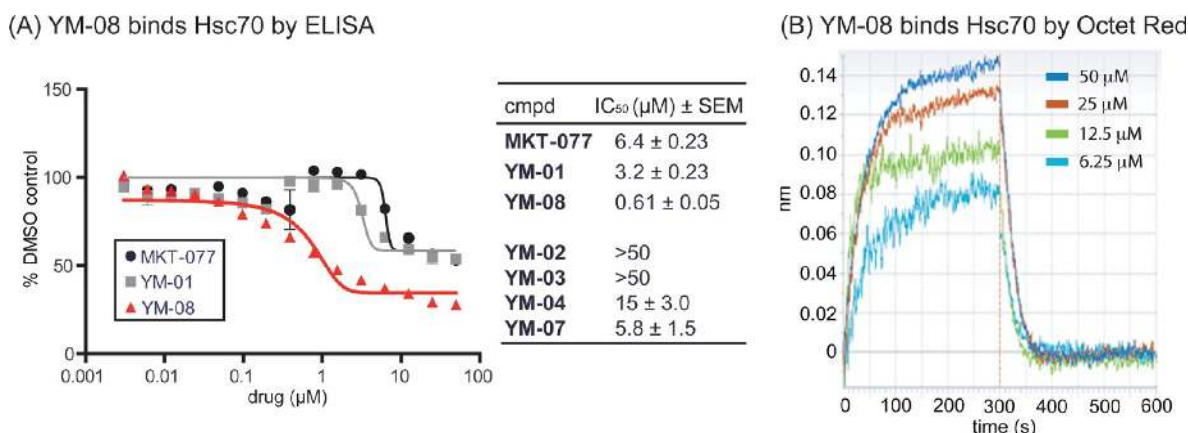## (B) YM-08 binds Hsc70 by Octet Red

Figure 2. YM-08 binds to Hsp70. (A) Binding of a biotinylated MKT-077 to immobilized human Hsc70 was measured by ELISA. Results are the average of experiments performed in triplicate, and error is SEM. (B) YM-08 binding to biotinylated Hsc70$_{NBD}$ was also measured by Octet Red. Fitting the binding curves gave a K_D value of ~2.3 μM. Similar results were obtained using full length Hsp72 (HSPA1). Results are representative of experiments performed in triplicate.

permeability. The resulting compound, YM-08 (Figure 1A), is predicted to have more favorable clogP (3.8) and tPSA (35.9) values.

In this study, we report the synthesis and initial characterization of YM-08. We found that YM-08 retained affinity for Hsp70 in vitro and that it selectively reduced pathogenic tau in brain slices. In mice, YM-08 crossed the BBB and maintained a brain/plasma (B/P) ratio greater than 0.25 for 18 h. Moreover, YM-08 was quickly cleared from the kidney, perhaps reducing the opportunity for renal damage. Thus, YM-08 may represent a suitable chemical scaffold for further development as a CNS-penetrant Hsp70 inhibitor.

■ RESULTS AND DISCUSSION

To initiate these studies, we first synthesized MKT-077 and its close derivative YM-01[20,21] using a previously reported synthetic route (Figure 1B).[32] Briefly, this synthesis progressed through reaction of 2-(methylthio)benzothiazole (**1**) with *p*-TsOMe to afford its methylthioiminium salt, which was subsequently condensed with rhodanine (**3**) to afford compound **4** (YM-02). Compound **4** was further activated by *p*-TsOMe to yield intermediate **5** (YM-03), followed by condensation with either 1,2-dimethylpyridin-1-ium (**6a**) or 1-ethyl-2-methylpyridin-1-ium (**6b**) to afford **7a** and **7b**. Final counterion exchange yielded MKT-077 and YM-01 in good overall yield (~25%). Adding to this series, we also condensed intermediates **4** and **6b** to produce a truncated analogue, YM-04, which lacks the benzothiazole group. Next, we synthesized the neutral compound, YM-08, via condensation of the common intermediate **4** with 1-((1,3-dioxoisoindolin-2-yl)methyl)-2-methylpyridin-1-ium bromide (**8**) to yield compound **9** (Figure 1C). Deprotection of **9** with aqueous ammonium hydroxide yielded YM-08 in ~25% overall yield. As another control, we generated YM-07, a neutral analogue of YM-04, using a previously reported route.[33]

We evaluated binding of these MKT-077 analogues to immobilized Hsp70 using a competitive ELISA. In this established assay,[21,34] a biotinylated version of MKT-077 is bound to immobilized human Hsc70 (HSPA8) and potential competitors are tested for their ability to block the interaction. We first confirmed that both MKT-077 and YM-01 could inhibit binding, with inhibition constant (IC_{50}) values of 6.4 $\pm$ 0.23 and 3.2 $\pm$ 0.23 μM, respectively. Interestingly, YM-08 had an apparent IC_{50}

of 0.61 $\pm$ 0.05 μM in the same assay, strongly suggesting that the charged pyridinium is not required for binding and that the pyridine may even be favored (Figure 2A). As further controls, we tested the truncated compounds YM-02, YM-03, YM-04, and YM-07. Removing the benzothiazole from YM-08 (compound YM-07) significantly weakened affinity (IC_{50} ~ 5.8 $\pm$ 1.5 μM; ~10-fold worse than YM-08), suggesting an important role for that group. Likewise, switching the pyridine of YM-07 to a cationic pyridinium (compound YM-04) further weakened affinity (IC_{50} ~ 15 $\pm$ 3 μM; ~2-fold worse than YM-07), re-enforcing the conclusion that the pyridine is preferred over the pyridinium. Finally, removing the ring altogether (compounds YM-02 and YM-03) abolished binding (IC_{50} > 50 μM) (Figure 2A). To confirm the binding of YM-08 in a separate experimental platform, we directly measured its affinity for immobilized Hsc70$_{NBD}$ and Hsp72 (HSPA1) by biolayer interferometry (BLI) and obtained K_D values of ~4 and 2 μM, respectively (Figure 2B). Together, these results show that YM-08 binds to Hsp70 and that both the benzothiazole and pyridine/pyridinium moieties are important for binding.

To further explore the interaction between YM-08 and Hsc70, we performed docking simulations in AUTODOCK 4.2 (see the Methods section). Specifically, YM-08 was docked to Hsc70$_{NBD}$ (PDB: 3C7N), revealing two best clusters (−6.0 and −5.6 kcal/mol, respectively) (Figure 3A and B) that were both predicted to position YM-08 in a cleft between subdomains IIA and IIB, adjacent to the nucleotide-binding site. This pocket is framed by a number of residues, including S208, S221, T222, D225, H227, and L228 (Figure 3C) that are known to be sensitive to addition of MKT-077.[23] When the side chains of these residues were allowed to freely rotate, they adjusted to define the YM08-binding pocket (see Figure 3A). In this orientation, the benzothiazole of YM-08 was predicted to access a deep cleft composed of hydrophobic and cationic residues (T12, K70, R71, R75, V81, Y148, T203, G223, and T225). This orientation is slightly offset from that adopted by MKT-077 (Figure 3D),[23] suggesting that, as suggested by the competition binding studies (see Figure 2A), the two molecules share a partially overlapping binding site.

Next, we wanted to test whether binding of YM-08 to Hsp70 might affect chaperone functions. MKT-077 analogues have been reported to modestly inhibit ATP hydrolysis, using a model Hsp70 system that includes yeast Hsp70 (Ssa1) and the stimulatory co-chaperone, Hlj1.[18,35] Using an identical assay system,
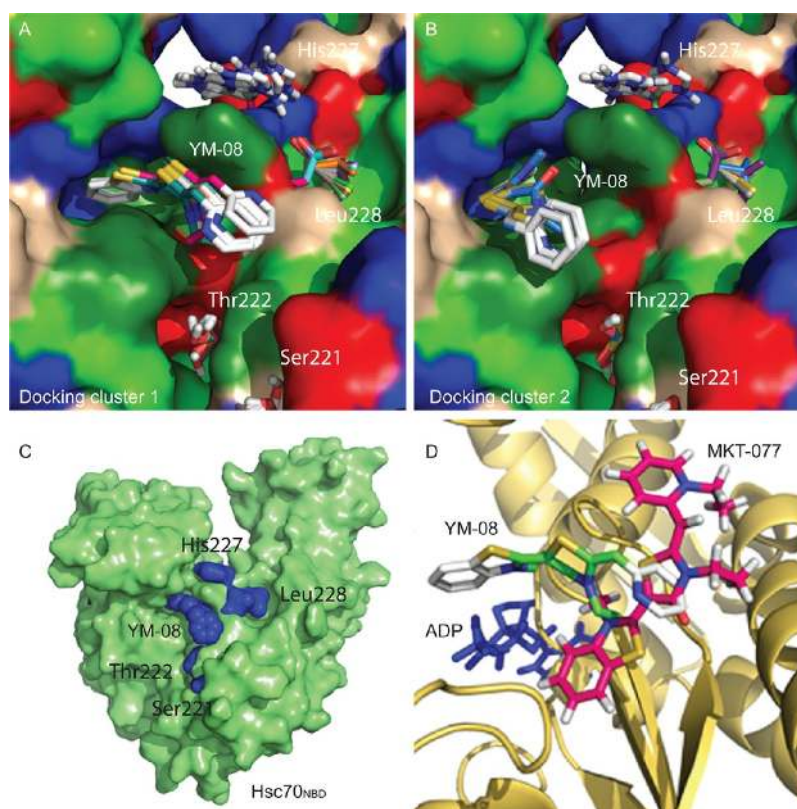
Figure 3. Docking of YM-08 to Hsc70. (A) Best cluster with an energy of −6.0 kcal/mol for its best binding member. The search box was restricted by the reported NMR shift perturbations from binding to MKT-077.[23] Protein colors are as follows. Green: A, C, F, I, L, M, P, V, W; dark green: T, Y; blue: H, K, R; red: D, E; peach: G, N, Q, S. (B) Second-best cluster with an energy of −5.6 kcal/mol for its best member. (C) Projected binding of YM-08 (best cluster) onto a surface representation of Hsc70 NBD. Residues responsive to MKT-077 are shown in blue and YM-08 is displayed as blue spheres. (D). MKT-077 (magenta) and YM-08 (light green) are predicted to bind partially overlapping pockets in Hsc70. ADP is shown in blue. Figure panels were generated using PyMOL.

we found that YM-08 also partially inhibited ATP turnover (Figure 4A). Interestingly, YM-08 only inhibited the Hlj1-stimulated ATPase activity, with minimal effect on the intrinsic ATPase activity of Ssa1 (Figure 4A). This profile is shared with other allosteric Hsp70 inhibitors.[17,18,34,36,37] As another test of chaperone function, we measured the effects of the compounds on the binding of Hsp70 to a misfolded protein. In previous work, MKT-077 stabilized the interaction between prokaryotic Hsp70 (DnaK) and denatured luciferase.[23] Briefly, this assay involves immobilizing unfolded luciferase in microtiter plates and measuring binding to DnaK.[34] Using this approach, we tested the MKT-077 analogues and found that MKT-077, YM-01, and YM-08 (50 μM) all significantly enhanced binding by ∼30% (Figure 4B). Conversely, the truncated molecules (YM-02, YM-03, YM-04, and YM-07) had reduced activity. To explore whether YM-08 might also enhance binding of Hsp70 to a more physiologically relevant substrate, we measured binding of tau to immobilized human Hsc70. In this configuration, YM-08 modestly enhanced the affinity of chaperone for the protein substrate (Figure 4B). Together, these studies show that YM-08 partially inhibits the enzymatic functions of Hsp70 family members and promotes tight binding to chaperone "clients".

Hsp70 inhibitors, including MKT-077, have been shown to accelerate degradation of tau and affect processing of other chaperone-dependent substrates in cells.[12,23,38−40] To determine whether YM-08 might also accelerated tau degradation, we treated HeLaC3 cells, which stably overexpress human 4R0N tau with compound. After 24 h, the levels of phosphorylated (p396/404)

tau and total tau were measured by Western blot. The results showed that YM-08 (30 μM) decreased the levels of pS396/404 and total tau by ∼40% and ∼60%, respectively (Figure 4C). This cellular activity is not as dramatic as that of MKT-077, which reduced tau levels by >80% at 30 μM (Figure 4D);[23] however, reducing tau by only ∼50% is predicted to provide benefits in some AD models.[4] Importantly, we also confirmed that, like MKT-077 and other Hsp70 inhibitors,[12,41,42] YM-08 did not induce a stress response, based on the unchanged levels of stress inducible Hsp72 (HSPA1) in the treated cell lysates (Figure 4C). Finally, we found that all of the truncated compounds had significantly reduced anti-tau activity (Figure 4D), consistent with the in vitro binding studies and the proposed importance of each of the three ring systems.

We then tested whether YM-08 might retain the anti-cancer activity of MKT-077. MTT assays showed that MKT-077 had EC_{50} values between 1.4 and 3.0 μM against MCF-7, MCF-10A, and MB-MDA-231 cells (Figure 4D). YM-01 had similar activity (EC_{50} values between 2.0 and 5.2 μM), while YM-08 had diminished potency, with EC_{50} values between 7.8 and 10.5 μM (Figure 4D). Notably, the truncated molecules tended to have poor activity (most EC_{50} values > 30 μM), consistent with the binding results. It is possible that the residual activity for YM-02 and YM-07, especially in MCF7 cells (Figure 4D), may arise from off-target effects.

Because MKT-077 binds to a dynamic, allosteric site on Hsp70 that is not overlapping with the nucleotide-binding cleft (see Figure 3) and is far removed from the peptide-binding region,

(A) YM-08 partially inhibits ATPase activity by an Hsp70 system
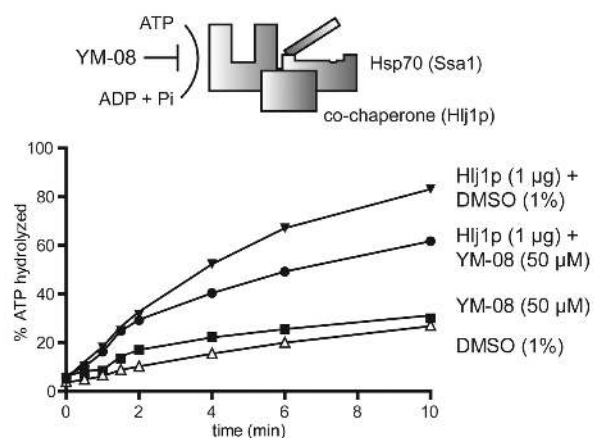
(C) YM-08 retains anti-tau activity in HeLaC3 cells
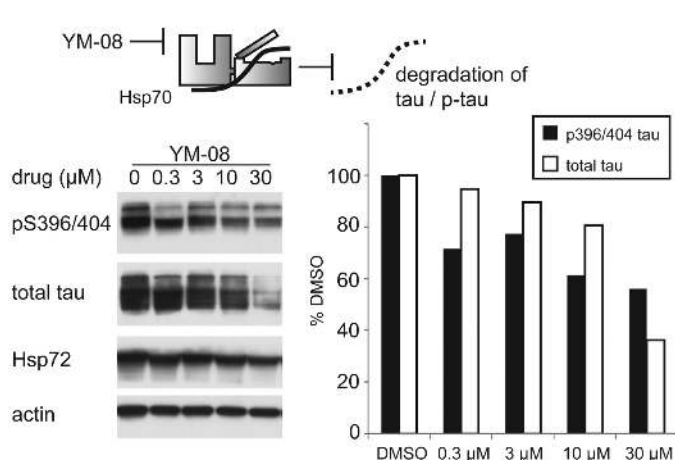
(B) YM-08 enhances binding to misfolded proteins *in vitro*.
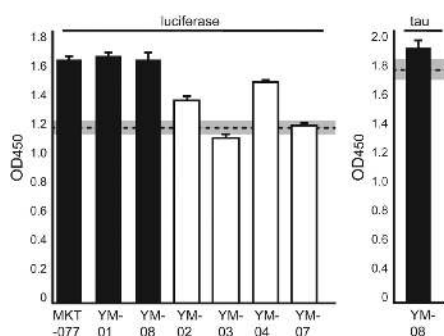
(D) Comparison of the biological activities of MKT-077, YM-08 and their analogs

compound	anti-tau (HeLaC3 cells)			cancer cell viability (EC$_{50}$ μM)		
	p-tau (%)	total tau (%)	EC$_{50}$ (μM)	MCF7	MCF10A	MDA-MB-231
MKT-077[a]	81	80	8.0 ± 1.3	2.2 ± 0.2	3.0 ± 0.2	1.4 ± 0.3
YM-01	88	89	3.2 ± 0.9	5.2 ± 0.8	3.3 ± 0.3	2.0 ± 0.2
YM-08	42	64	15 ± 3.1	10.5 ± 1.9	7.8 ± 0.7	8.5 ± 1.4
YM-02	12	21	>30	5.8 ± 1.9	13.8 ± 2.2	>30
YM-03	39	40	22 ± 6.5	>30	>30	>30
YM-04	0	0	>30	>30	>30	>30
YM-07	5	7	>30	6.5 ± 2.9	>30	>30

[a] tau data from reference 23.

Figure 4. YM-08 retains anti-Hsp70 activities in vitro and in cells. (A) Single turnover ATPase assays were performed using purified yeast Ssa1p and Hlj1p. Results are the average of experiments performed in triplicate, and error bars represent SEM. (B) Binding of DnaK to denatured luciferase (or human 4R0N tau) and the effects of MKT-077 analogues on the apparent affinity. Results are the average of triplicates, and error is SEM. The dashed line is a DMSO control, and the gray box is the error of the control. All compounds were tested at 50 μM. *p*-value < 0.01. (C) Western blots of treated HeLaC3 cells, showing that YM-08 reduced phospho (p396/404) and total tau. Quantification of the results was performed in NIH Image J, and the results are shown. (D) Summary of the anti-tau and anti-cancer activity of MKT-077, YM-08, and their analogues. The error is SEM.

we did not expect direct correlations between the calculated binding affinity values and any effects on chaperone functions or cellular activity. Consistent with this idea, the preliminary structure–activity relationships (SARs) for this chemical series were complex, especially when comparing in vitro values to potency in cellular assays. For example, the truncated molecule YM-02 had weak affinity (IC$_{50}$ > 50 μM) for Hsp70 in vitro (see Figure 2A), yet it has some residual activity in the luciferase binding (Figure 4B) and cell-based anti-tau assays (Figure 4D). Also, YM-08 had a superior affinity for Hsc70 (see Figure 2), but reduced anti-tau activity in cells when compared to the parent molecule MKT-077 (see Figure 4C). Regardless of the allosteric/mechanistic origins of these differences, the results suggest that removing either the benzothiazole (e.g., YM-07) or the pyridine/pyridinium (e.g., YM-02) reduced potency across all of the assay formats. Also, the results support the conservative conclusions that YM-08 retained binding to Hsp70 and that it modestly reduced tau levels in cultured cells. Additional structural and mechanistic studies, along with an expanded collection of analogues, will be required to achieve quantitative SAR.

Although YM-08 had relatively modest effects in the HeLaC3 model of tau accumulation, we wanted to test its activity in a more physiological system. Brain slice cultures from transgenic mice that express mutated tau[13] were treated for 6 h with YM-08, and the levels of total- and pS396/404 tau measured by Western blots. At both 30 and 100 μM concentrations, YM-08 reduced phospho-tau in this model (Figure 5A), consistent with the cell culture model. Thus, YM-08 also reduced the levels of disease-associated tau in a neuronal model. Recent findings suggest that Hsp70 binds tau immediately after its release from microtubules.[10] To test whether YM-08 might selectively reduce tau after microtubule disruption, we cultured brain slices from wild type mice and treated them with YM-08 plus the microtubule destabilizer, nocodazole. Treatment of these cultures with YM-08 alone did not significantly reduce tau levels (Figure 5B), consistent with the idea that most tau in nonpathogenic conditions is associated with microtubules and not available for removal through the Hsp70 system. However, acute disruption of the microtubule network with nocodazole dramatically increased the potency of YM-08 and led to decreased levels of both total and phospho-tau (Figure 5B). Together, these studies add to growing evidence that Hsp70 selectively identifies tau variants that are not associated with the normal microtubule network, likely minimizing their aggregation and proteotoxicity.[6,7,10] Further, these results suggest that enhancing the affinity of Hsp70 for tau, using molecules such as YM-08, promotes proper tau triage.
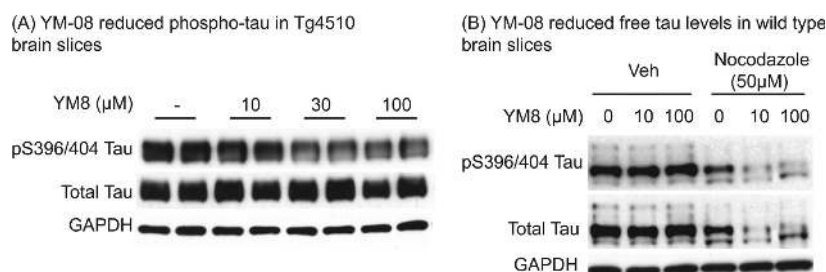
Figure 5. YM-08 reduces pathogenic tau levels in brain slices. (A) Brain slices from transgenic P301L tau mice (Tg4510) were treated for 6 h with YM-08 and the levels of phospho- and total tau were measured. (B) Tau levels were unchanged in wild type brain slices treated with YM-08, but disruption of the microtubules with nocodozole promoted the ability of YM-08 to reduce total and phospho-tau levels.
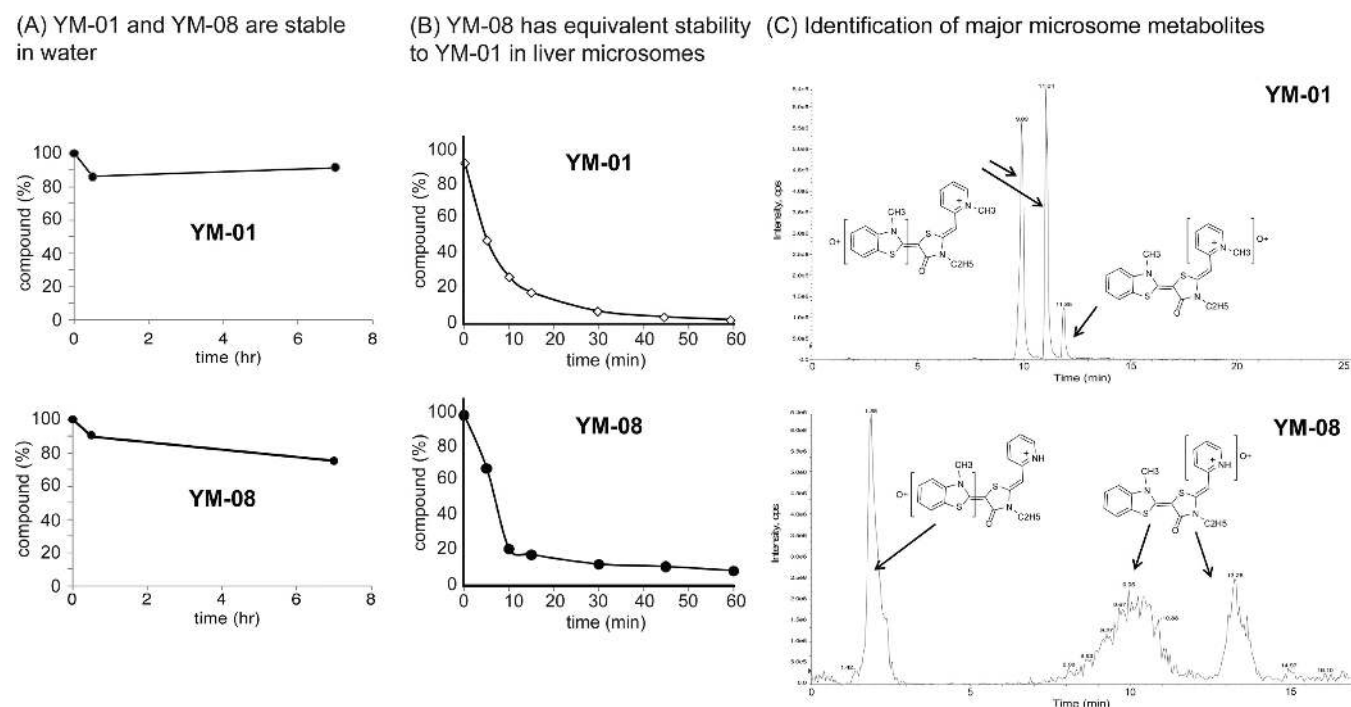

Figure 6. Initial characterization of YM-08 stability and metabolism. (A) Both YM-01 and YM-08 (100 μM) were relatively stable in water, as determined using LC-MS. (B) YM-01 and YM-08 were treated with human liver microsomes and (C) the major metabolites identified by LC-MS/MS. The $t_{1/2}$ values were both approximately 4 min, and two major oxidation products were found.

Next, we wanted to explore the relative stability and pharmacokinetics of a charged (YM-01) and neutral (YM-08) analogue. To test their stability in aqueous media, we incubated YM-01 or YM-08 (100 μM) in water at room temperature and found that both compounds were stable for at least 8 h (Figure 6A). As an initial examination of the metabolism of YM-08, we studied its stability in the presence of human liver microsomes. In this system, both YM-01 and YM-08 were rapidly metabolized ($t_{1/2}$ values of ~2−4 min) (Figure 6B), largely by oxidation on the benzothiazole and pyridine ring systems (Figure 6C). MKT-077 has a similar reported rate of metabolism.[30] Together, these results indicate that replacement of the charged pyridinium did not significantly impact metabolic or aqueous stability.

We then tested the initial pharmacokinetics (PK) of YM-01 and YM-08 in CD1 mice. YM-01 (20 mg/kg; saline) was prevalent in the kidney at both 0.16 and 1 h after i.v. injection, but it lacked detectable brain penetration (Figure 7A). This result is consistent with the known properties of MKT-077.[30] In contrast, YM-08 (10 mg/kg; 10% DMSO/saline (v/v) i.v.) was abundant in the brain at 0.16 h, with reduced retention in the kidney and

rapid clearance from all compartments (Figure 7A). These results suggested that YM-08 was BBB permeable, consistent with its design. While these preliminary PK results were promising, YM-08 was only marginally soluble in the DMSO/saline mixture, so we reformulated YM-08 in a Cremophor mixture (see the Methods section) and performed a more definitive analysis of the brain and plasma levels over time in CD1 mice. After a single 6.6 mg/kg dose delivered i.v., the peak brain concentration of YM-08 was 4 μg/g (Figure 7B) and the B/P ratio was approximately 0.25 for 18 h (Figure 7C). Typically, B/P values greater than 0.3 are considered promising for CNS leads,[43] suggesting that, with additional optimization, YM-08 could be a promising analogue. It is not yet clear how much tau levels need to be reduced to achieve therapeutic effects in disease models, but the area-under-the-curve (AUC$_{inf}$) for YM-08 in the brain was 0.26 μg·h/g and the AUC$_{inf}$ in plasma was 13.6 μg·h/mL. The terminal halftime in the brain ($t_{1/2;brain}$) was 6.8 h and the $t_{1/2;plasma}$ was 9.8 h. The clearance rate in mice was slower than that observed in the human liver microsome studies (see Figure 5B), suggesting the potential for differences in the metabolism of YM-08 between these organisms.

(A) Initial pharmacokinetics of YM-01 and YM-08

YM-01 (20 mg/kg ; i.v.)

hour	plasma (ng/mL)	brain (ng/g)	kidney (ng/g)
0.16	359	0	74378
1	324	0	63231

YM-08 (10 mg/kg ; i.v.)

hour	plasma (ng/mL)	brain (ng/g)	kidney (ng/g)
0.16	1600	5743	7231
1	14.8	n.a.	55.2

(B) YM-08 (6.6 mg/kg) is BBB permeable
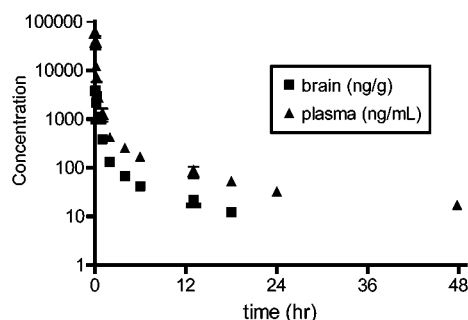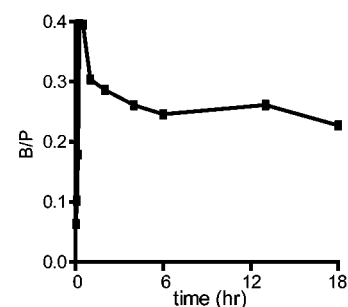
(C) YM-08 maintains B/P ~0.25 for 18 hrs

Figure 7. Pharmacokinetics of YM-08 in CD1 mice. (A) Initial pharmacokinetics and biodistribution of YM-01 and YM-08. Compounds were suspended in buffered saline (YM-01) or 10% DMSO/saline (YM-08) and injected at 20 and 10 mg/kg, respectively. YM-08 was not soluble in saline or 10% DMSO/saline at 20 mg/kg. The levels of YM-08 in the brain at 1 h after injection could not be accurately determined (n.a.) because its value was outside the calibration curve. (B) More detailed study of YM-08 in plasma and brain was performed after single (100 μL) i.v. injection (6.6 mg/kg) in 30% water; 5% Cremophor, 5% ethanol, 60% PBS. Results are average from data acquired from three female mice. (C) YM-08 maintains a B/P ratio of nearly 0.25 for 18 h.

In conclusion, we have synthesized a derivative of MKT-077 and found that it binds Hsp70, inhibits ATP turnover, and enhances binding of Hsp70 to its "clients". Although YM-08 was somewhat less effective than MKT-077 in anti-tau and anti-cancer assays, it was BBB permeable and was not retained in the kidney. Thus, we have overcome some of the hurdles in progression of this chemical series toward use in studying tauopathies. However, further advancement of the series will require additional optimization of metabolic stability, solubility, and potency. The metabolite identification studies (see Figure 5C) may provide useful guidance on modifications that enhance metabolic stability. With further work, YM-08 could serve as a promising scaffold for the development of CNS penetrant Hsp70 inhibitors.

■ METHODS

General Methods. Reagents were purchased from Sigma-Aldrich, Alfa Aesar, or TCI America, and directly used without further purification. NMR experiments were carried out using a 600 MHz Varian NMR apparatus. Mass spectrometry data were collected on Micromass LCT time-of-flight mass spectrometer with electrospray ionization. Mammalian Hsp70 proteins were expressed, purified, and handled as previously described.[44]

Synthesis. MKT-077 analogues were synthesized as previously described (see the Supporting Information for detailed synthesis and characterization of YM-01, YM-08, and analogues).[32] For the in vitro experiments, stock solutions were prepared in DMSO (100 mM).

ELISA Competitive Binding Assay. A sample of Hsc70 (50 μL; 0.06 mg/mL) was immobilized in a clear flat-bottom 96-well plate in MES buffer (50 mM 2-(N-morpholino)ethanesulfonic acid, pH 5.2) at 37 °C overnight. After discarding the excess protein solution, each well was washed three times with 150 μL of TBS-T buffer (25 mM Tris, 140 mM NaCl, 2.7 mM KCl, 0.01% Tween-20, pH 7.4). Then, 1 μL of compound (1% DMSO) was diluted into 24 μL of binding buffer (100 mM Tris, 20 mM KCl, 6 mM MgCl$_2$, 0.01% Triton-X100) and incubated at room temperature for 30 min. Biotin labeled MKT-077 (final concentration 1 μM; 25 μL) was subsequently added into each well and the mixture was incubated at room temperature for another 3 h. The wells were washed with 150 μL of TBS-T buffer three times prior to blocking with 100 μL of 3% bovine serum albumin (BSA) in TBS-T buffer for 5 min at room temperature. After the removal of the BSA solution, 50 μL of HRP-streptavidin (Pierce Biotechnology, 1:50 000 TBS-T dilution) solution was added and the plates were incubated at room temperature for 1 h. The HRP-streptavidin solution was removed, and wells were washed three times with 150 μL of TBS-T. TMS substrate (Cell Signaling Technology 100 μL) was added into each well and

incubated at room temperature until a visible blue color was shown in wells (~20 min). HCl stop solution (1 M) was then added into each well to yield a yellow solution, and the absorbance at 450 nm was recorded on a SpectraMax M5 instrument (Molecular Devices). In control experiments, the biotinylated MKT-077 bound to human Hsp72 (4.9 ± 0.8 μM) and DnaK (16.7 ± 3.1 μM) with similar affinities to human Hsc70 (6.4 ± 0.23 μM), reinforcing the similarity among the Hsp70 family members in the reported MKT-077 binding site.[23]

Biolayer Interferometry (Octet Red). Biotinylated human Hsc70$_{NBD}$ or full length Hsp72 was first immobilized on super streptavidin biosensors (ForteBio, 18-5057) as follows: biosensors were soaked with MG buffer (100 mM Tris base, 20 mM KCl, 6 mM MgCl$_2$, 0.01% Triton X-100, pH 7.4) for 10 min before moving them to wells containing 200 μL of either 100 μg/mL biotinylated proteins or 100 μg/mL biocytin for 60 min. The free streptavidin sites were subsequently quenched with 100 μg/mL biocytin for 10 min. The biosensors were washed with MG buffer for 5 min prior to beginning the binding experiments. The association and disassociation steps were carried out in MG buffer with a constant 10% DMSO concentration. All steps were performed at room temperature and with 1000 rpm rotary shaking. Compounds were allowed to associate with the biosensor surface for 5 min and then to disassociate with the biosensor for 5 min. Compounds were tested from low to high concentration in duplicates. Biocytin-loaded biosensors were used to correct the baseline drifts. The apparent affinities of YM-08 for Hsc70$_{NBD}$ and Hsp72 were calculated from both equilibrium measurements and global fits of the k_{on} and k_{off} values, yielding similar values.

Molecular Docking. AUTODOCK-4.2 was used for the docking of YM-08 to Hsc70$_{NBD}$ in complex with yeast Hsp110 (PDB code 3C7N). This target was chosen because it is the only Hsp70-like protein structure available that is in complex with ADP and Mg^{2+}. Prior to docking, the Hsp110 sequence was removed and the remaining Hsc70$_{NBD}$, ADP, and Mg^{2+} were minimized using DOCK6 and Amber force field parameters as previously described.[23] Then, using a 0.2 Å resolution AUTODOCK grid box that was centered around the known MKT-077 binding site, we performed a Lamarkian genetic algorithm with the following parameters: GA runs = 100, initial population size = 1500, max number of evaluations = long, max number of surviving top individuals = 1, gene mutation rate = 0.02, rate of crossover = 0.8, GA crossover mode = two points, Caushy distribution mean for gene mutation = 0, Cauchy distribution variance for gene mutation = 1, number of generations for picking worst individuals = 10. The docked structures were clustered and then evaluated using PyMOL. All calculations were completed on a Apple MacBookPro computer equipped with a 64-bit 2.4 GHz Intel Core 2 Duo processor running MacOSX 10.6.8.

ATPase Assay. Single turnover ATPase assays were performed as previously described.[18,35] Briefly, the yeast Hsp70, Ssa1p (~0.2 μM), was prebound to α-[^{32}P]ATP. The hydrolysis of ATP in the presence or

absence of an equimolar amount of Hlj1 was measured by monitoring the generation of α-[^{32}P]ADP by thin layer chromatography (TLC).

Luciferase Binding. Binding of prokaryotic Hsp70 (DnaK) to denatured luciferase was measured as previously described.[34] Briefly, firefly luciferase (0.2 mg/mL) was proteolyzed with trypsin and immobilized in 96-well microtiter plates. After washing, the binding of luciferase to DnaK (500 nM) was measured using an anti-DnaK antibody and HRP secondary antibody. A similar strategy was used to monitor binding of human Hsc70 to tau, as previously described.[44]

Cell and Brain Slice Culture. MCF7 cells were cultured in Dulbecco's modified Eagle's medium (DMEM) with 10% fetal bovine serum (Invitrogen) and 1% penicillin-streptomycin (pen-strep; Invitrogen). MCF10A cells were cultured in DMEM/F-12 with 10% FBS, 1% pen-strep, 5% horse serum (Invitrogen), 500 ng/mL hydrocortisone (Sigma), 25 ng/mL epidermal growth factor (R&D Systems), 10 μg/mL bovine insulin (Sigma), and 100 ng/mL cholera toxin (Sigma). HeLaC3 cells were cultured in OptiMem (Invitrogen) with 10% FBS and 1% pen-strep. MDA-MB-231 cells were cultured in DMEM with 10% FBS, 1% pen-strep, and 1% nonessential amino acids (Invitrogen). All cells were maintained at 37 °C with 5% CO_2 in a humidified atmosphere. Brain slice cultures were created as previously described[12] and treated for 6 h with YM-08 at the indicated concentration.

Cell Survival Assay. Cell viability was determined using a methyl thiazoyl tetrazolium (MTT) colorimetric assay (ATCC, catalog number 30-1010K) with the following modifications. Briefly, cells (5×10^3) were plated into 96-well assay plates in 0.1 mL of media and allowed to attach overnight. The cells were then treated with compound at various concentrations in 0.2 mL of fresh media. After the 72 h incubation period, cells were washed in PBS ($3 \times 100 \mu$L), and 10 μL of MTT reagent was added with 100 μL of fresh media. The cells were then incubated for 4 h in a humidified chamber at 37 °C with 5% CO_2. Insoluble formazan crystals were solubilized by addition of 0.1 mL of detergent solution (4 h at room temperature in the dark). Resulting colored solutions were then quantified at an absorbance of 570 nm.

Pharmacokinetics General Methods. Mouse liver microsomes (20 mg/mL) containing cytochrome P450, cytochrome b5, and NADPH-cytochrome c reductase were purchased from XenoTech, LLC (Lenexa, KS). β-NADPH, $MgCl_2$, and 0.1 M phosphate buffer were obtained from Sigma-Aldrich (St. Louis, MO). High-performance liquid chromatography (HPLC)-grade acetonitrile was purchased from Thermo Fisher Scientific (Waltham, MA). HPLC water was purified using a Milli-Q water system (Millipore Corporation, Billerica, MA).

Characterization of Metabolites. To identify metabolites of YM-01 and YM-08, metabolized samples and two negative controls were prepared. In the metabolized samples, 10 μM YM-01 or YM-08 was incubated with mouse liver microsomes (1 mg/mL) in 0.1 M phosphate buffer containing 3.3 mM $MgCl_2$ and 1 mM β-NADPH at 37 °C for 2 h. In the first control, 10 μM YM-08 was incubated with 1 mg/mL of boiled microsomes (100 °C for 5 min) in the same buffer. In the second control, neither YM-08 nor microsomes were added to the buffer. After 2 h incubation, reactions were terminated by adding one volume of ice-cold acetonitrile. The supernatants were collected after precipitating protein via centrifugation at 14 000 rpm for 10 min and then subjected to LC-MS/MS analysis. In the second control, YM-01 or YM-08 (5 μM) was added prior to LC-MS/MS analysis. In the analysis, multiple-reaction monitoring (MRM) mode was employed to identify the potential metabolites. Based on the precursor and fragment ions, the MRM ion transition list of possible metabolites was generated by Metabolite ID software (Applied Biosystems), which accounts for 40 common biotransformation processes. Only the peaks that were detected in the sample but absent in both negative controls were determined to be the metabolites of YM-08. To characterize the metabolites of YM-08, the peaks were selected individually and subjected to MS^2 scan to obtain fragments.

Pharmacokinetic sampling. Female CD-1 mice (25–30 g in body weight) were purchased from Charles River Laboratories (Wilmington, MA). Mice were treated with 6 mg/kg YM-08 through the tail-vein injection. The plasma and brain were collected at 0.016, 0.08, 0.16, 0.25, 0.5, 1, 2, 4, 6, 13, 18, 24, and 48 h after drug administration. Whole blood samples were drawn through the cardiac puncture using a heparinized

syringe with a 22 gauge needle, followed by centrifugation at 3000g for 10 min at 4 °C to obtain plasma. Collected tissues were washed with PBS, immediately frozen using liquid nitrogen, and stored at −80 °C until further analysis. Tissue homogenates were prepared by adding PBS (1:5 w/v, homogenate/PBS) and homogenized for 3 min. Compound was extracted from 100 μL of sample by adding 300 μL of acetonitrile containing 50 ng/mL IS, followed by vortexing for 3 min. The supernatant was collected and subjected to LC-MS/MS analysis.

LC/MS/MS Analysis. The separation of YM-08 and internal standard was performed using an Agilent 1200 HPLC system (Agilent Technologies, Santa Clara, CA) and Zobarx SB-C18 column (2.1 × 50 mm, 3.5 μm) (Agilent Technologies). YM-08 was dissolved from solid in 30% water, 5% Cremophor, 5% ethanol, and 60% phosphate buffered saline. The compounds were eluted with an fixed gradient of 20% solvent A and 80% solvent B. Solvent A consisted of 0.1% (v/v) glacial acetic acid in water, and solvent B consisted of 0.1% (v/v) glacial acetic acid in acetonitrile. After injecting 10 μL of samples into the HPLC system, the elution was performed over 2 min at a flow rate of 0.4 mL/min. The YM-08 and MKT-077 eluents were detected using QTRAP 3200 mass spectrometer (Applied Biosystems/MDS Sciex, Foster City, CA) equipped with an electrospray ionization source (ESI). The temperature of ESI was set at 650 °C, and curtain gas, gas 1, and gas 2 were set to 30, 50, and 50 units, respectively. A positive voltage at 5500 V was applied through ESI to convert the eluents to ions in the form of MH$^+$. The ions were detected using a MRM mode. The ion transitions from the precursor ion ($m/z = 368$) to the fragment ion ($m/z = 222$) and from the precursor ion ($m/z = 396$) to the fragment ion ($m/z = 175$) were used to detect YM-08 and IS, respectively.

■ ASSOCIATED CONTENT

Ⓢ Supporting Information

Additional figures and details of compound characterization. This material is available free of charge via the Internet at http://pubs.acs.org.

■ AUTHOR INFORMATION

Corresponding Author

*Mailing address: University of Michigan, Life Sciences Institute, 210 Washtenaw Ave., Ann Arbor, MI 48109-2216. E-mail: gestwick@umich.edu.

Notes

The authors declare no competing financial interests.

Author Contributions

Y.M., X.L., H-F.L., U.K.J., S.R.S., S.P.S., and Z.T.Y. performed experiments. Y.M., X.L., H-F.L., U.K.J., S.R.S., S.P.S., Z.T.Y., J.L.B., C.A.D., D.S., and J.E.G. interpreted results and prepared the manuscript.

■ ACKNOWLEDGMENTS

■ REFERENCES

(1) Lee, V. M., Goedert, M., and Trojanowski, J. Q. (2001) Neurodegenerative tauopathies. *Annu. Rev. Neurosci.* 24, 1121−1159.

(2) Oddo, S., Caccamo, A., Shepherd, J. D., Murphy, M. P., Golde, T. E., Kayed, R., Metherate, R., Mattson, M. P., Akbari, Y., and LaFerla, F. M. (2003) Triple-transgenic model of Alzheimer's disease with plaques and tangles: intracellular Abeta and synaptic dysfunction. *Neuron 39*, 409−421.

(3) Roberson, E. D., Scearce-Levie, K., Palop, J. J., Yan, F., Cheng, I. H., Wu, T., Gerstein, H., Yu, G. Q., and Mucke, L. (2007) Reducing endogenous tau ameliorates amyloid beta-induced deficits in an Alzheimer's disease mouse model. *Science 316*, 750−754.

(4) Vossel, K. A., Zhang, K., Brodbeck, J., Daub, A. C., Sharma, P., Finkbeiner, S., Cui, B., and Mucke, L. (2011) Tau reduction prevents Abeta-induced defects in axonal transport. *Science 330*, 198.

(5) Wang, Y., Garg, S., Mandelkow, E. M., and Mandelkow, E. (2010) Proteolytic processing of tau. *Biochem. Soc. Trans. 38*, 955−961.

(6) Dickey, C. A., and Petrucelli, L. (2006) Current strategies for the treatment of Alzheimer's disease and other tauopathies. *Expert Opin. Ther. Targets 10*, 665−676.

(7) Miyata, Y., Koren, J., Kiray, J., Dickey, C. A., and Gestwicki, J. E. (2011) Molecular chaperones and regulation of tau quality control: strategies for drug discovery in tauopathies. *Future Med. Chem. 3*, 1523−1537.

(8) Evans, C. G., Chang, L., and Gestwicki, J. E. (2010) Heat shock protein 70 (hsp70) as an emerging drug target. *J. Med. Chem. 53*, 4585−4602.

(9) Voss, K., Combs, B., Patterson, K. R., Binder, L. I., and Gamblin, T. C. (2012) Hsp70 alters tau function and aggregation in an isoform specific manner. *Biochemistry 51*, 888−898.

(10) Jinwal, U. K., O'Leary, J. C., 3rd, Borysov, S. I., Jones, J. R., Li, Q., Koren, J., 3rd, Abisambra, J. F., Vestal, G. D., Lawson, L. Y., Johnson, A. G., Blair, L. J., Jin, Y., Miyata, Y., Gestwicki, J. E., and Dickey, C. A. (2010) Hsc70 rapidly engages tau after microtubule destabilization. *J. Biol. Chem. 285*, 16798−16805.

(11) Wang, Y., Martinez-Vicente, M., Kruger, U., Kaushik, S., Wong, E., Mandelkow, E. M., Cuervo, A. M., and Mandelkow, E. (2010) Synergy and antagonism of macroautophagy and chaperone-mediated autophagy in a cell model of pathological tau aggregation. *Autophagy 6*, 182−183.

(12) Jinwal, U. K., Miyata, Y., Koren, J., 3rd, Jones, J. R., Trotter, J. H., Chang, L., O'Leary, J., Morgan, D., Lee, D. C., Shults, C. L., Rousaki, A., Weeber, E. J., Zuiderweg, E. R., Gestwicki, J. E., and Dickey, C. A. (2009) Chemical manipulation of hsp70 ATPase activity regulates tau stability. *J. Neurosci. 29*, 12079−12088.

(13) O'Leary, J. C., 3rd, Li, Q., Marinec, P., Blair, L. J., Congdon, E. E., Johnson, A. G., Jinwal, U. K., Koren, J., 3rd, Jones, J. R., Kraft, C., Peters, M., Abisambra, J. F., Duff, K. E., Weeber, E. J., Gestwicki, J. E., and Dickey, C. A. (2010) Phenothiazine-mediated rescue of cognition in tau transgenic mice requires neuroprotection and reduced soluble tau burden. *Mol. Neurodegener. 5*, 45.

(14) Congdon, E. E., Wu, J. W., Myeku, N., Figueroa, Y. H., Herman, M., Marinec, P. S., Gestwicki, J. E., Dickey, C. A., Yu, W. H., and Duff, K. (2012) Methylthioninium chloride (methylene blue) induces autophagy and attenuates tauopathy in vitro and in vivo. *Autophagy 8*, 609−622.

(15) Patury, S., Miyata, Y., and Gestwicki, J. E. (2009) Pharmacological targeting of the Hsp70 chaperone. *Curr. Top. Med. Chem. 9*, 1337−1351.

(16) Brodsky, J. L., and Chiosis, G. (2006) Hsp70 molecular chaperones: emerging roles in human disease and identification of small molecule modulators. *Curr. Top. Med. Chem. 6*, 1215−1225.

(17) Wisen, S., Bertelsen, E. B., Thompson, A. D., Patury, S., Ung, P., Chang, L., Evans, C. G., Walter, G. M., Wipf, P., Carlson, H. A., Brodsky, J. L., Zuiderweg, E. R., and Gestwicki, J. E. (2010) Binding of a small molecule at a protein-protein interface regulates the chaperone activity of hsp70-hsp40. *ACS Chem. Biol. 5*, 611−622.

(18) Fewell, S. W., Smith, C. M., Lyon, M. A., Dumitrescu, T. P., Wipf, P., Day, B. W., and Brodsky, J. L. (2004) Small molecule modulators of endogenous and co-chaperone-stimulated Hsp70 ATPase activity. *J. Biol. Chem. 279*, 51131−51140.

(19) Wadhwa, R., Sugihara, T., Yoshida, A., Nomura, H., Reddel, R. R., Simpson, R., Maruta, H., and Kaul, S. C. (2000) Selective toxicity of MKT-077 to cancer cells is mediated by its binding to the hsp70 family protein mot-2 and reactivation of p53 function. *Cancer Res. 60*, 6818−6821.

(20) Koren, J., 3rd, Miyata, Y., Kiray, J., O'Leary, J. C., 3rd, Nguyen, L., Guo, J., Blair, L. J., Li, X., Jinwal, U. K., Cheng, J. Q., Gestwicki, J. E., and Dickey, C. A. (2012) Rhodacyanine derivative selectively targets cancer cells and overcomes tamoxifen resistance. *PLoS ONE 7*, e35566.

(21) Wang, A. M., Miyata, Y., Klinedinst, S., Peng, H.-M., Chu, J. C., Komiyama, T., Pratt, W. B., Oswaw, Y., Collins, C. A., Gestwicki, J. E., and Lieberman, A. P. (2013) Allosteric activation of Hsp70 binding promotes polyglutamine androgen receptor clearance and rescues toxicity in a Drosophila model of SBMA. *Nat. Chem. Biol. 9*, 112−118.

(22) Deocaris, C. C., Widodo, N., Shrestha, B. G., Kaur, K., Ohtaka, M., Yamasaki, K., Kaul, S. C., and Wadhwa, R. (2007) Mortalin sensitizes human cancer cells to MKT-077-induced senescence. *Cancer Lett. 252*, 259−269.

(23) Rousaki, A., Miyata, Y., Jinwal, U. K., Dickey, C. A., Gestwicki, J. E., and Zuiderweg, E. R. (2011) Allosteric drugs: the interaction of antitumor compound MKT-077 with human Hsp70 chaperones. *J. Mol. Biol. 411*, 614−632.

(24) Koya, K., Li, Y., Wang, H., Ukai, T., Tatsuta, N., Kawakami, M., Shishido, and Chen, L. B. (1996) MKT-077, a novel rhodacyanine dye in clinical trials, exhibits anticarcinoma activity in preclinical studies based on selective mitochondrial accumulation. *Cancer Res. 56*, 538−543.

(25) Chiba, Y., Kubota, T., Watanabe, M., Otani, Y., Teramoto, T., Matsumoto, Y., Koya, K., and Kitajima, M. (1998) Selective antitumor activity of MKT-077, a delocalized lipophilic cation, on normal cells and cancer cells in vitro. *J. Surg. Oncol. 69*, 105−110.

(26) Modica-Napolitano, J. S., Koya, K., Weisberg, E., Brunelli, B. T., Li, Y., and Chen, L. B. (1996) Selective damage to carcinoma mitochondria by the rhodacyanine MKT-077. *Cancer Res. 56*, 544−550.

(27) Britten, C. D., Rowinsky, E. K., Baker, S. D., Weiss, G. R., Smith, L., Stephenson, J., Rothenberg, M., Smetzer, L., Cramer, J., Collins, W., Von Hoff, D. D., and Eckhardt, S. G. (2000) A phase I and pharmacokinetic study of the mitochondrial-specific rhodacyanine dye analog MKT 077. *Clin. Cancer Res. 6*, 42−49.

(28) Propper, D. J., Braybrooke, J. P., Taylor, D. J., Lodi, R., Styles, P., Cramer, J. A., Collins, W. C., Levitt, N. C., Talbot, D. C., Ganesan, T. S., and Harris, A. L. (1999) Phase I trial of the selective mitochondrial toxin MKT077 in chemo-resistant solid tumours. *Ann. Oncol. 10*, 923−927.

(29) Weisberg, E. L., Koya, K., Modica-Napolitano, J., Li, Y., and Chen, L. B. (1996) In vivo administration of MKT-077 causes partial yet reversible impairment of mitochondrial function. *Cancer Res. 56*, 551−555.

(30) Tatsuta, N., Suzuki, N., Mochizuki, T., Koya, K., Kawakami, M., Shishido, T., Motoji, N., Kuroiwa, H., Shigematsu, A., and Chen, L. B. (1999) Pharmacokinetic analysis and antitumor efficacy of MKT-077, a novel antitumor agent. *Cancer Chemother. Pharmacol. 43*, 295−301.

(31) Pajouhesh, H., and Lenz, G. R. (2005) Medicinal chemical properties of successful central nervous system drugs. *NeuroRx 2*, 541−553.

(32) Nishigaki, J. (Fuji Film Corporation) Novel rhodacyanine intermediates and its application for dye synthesis. Japanese Patent 2004359801, Dec 24th, 2004.

(33) Pudhom, K., Kasai, K., Terauchi, H., Inoue, H., Kaiser, M., Brun, R., Ihara, M., and Takasu, K. (2006) Synthesis of three classes of rhodacyanine dyes and evaluation of their in vitro and in vivo antimalarial activity. *Bioorg. Med. Chem. 14*, 8550−8563.

(34) Miyata, Y., Chang, L., Bainor, A., McQuade, T. J., Walczak, C. P., Zhang, Y., Larsen, M. J., Kirchhoff, P., and Gestwicki, J. E. (2011) High-throughput screen for Escherichia coli heat shock protein 70 (Hsp70/DnaK): ATPase assay in low volume by exploiting energy transfer. *J. Biomol. Screening 15*, 1211−1219.

(35) Chiang, A. N., Valderramos, J. C., Balachandran, R., Chovatiya, R. J., Mead, B. P., Schneider, C., Bell, S. L., Klein, M. G., Huryn, D. M., Chen, X. S., Day, B. W., Fidock, D. A., Wipf, P., and Brodsky, J. L. (2009) Select pyrimidinones inhibit the propagation of the malarial parasite, Plasmodium falciparum. *Bioorg. Med. Chem. 17*, 1527−1533.

(36) Chang, L., Miyata, Y., Ung, P. M., Bertelsen, E. B., McQuade, T. J., Carlson, H. A., Zuiderweg, E. R., and Gestwicki, J. E. (2011) Chemical

screens against a reconstituted multiprotein complex: myricetin blocks DnaJ regulation of DnaK through an allosteric mechanism. *Chem. Biol.* *18*, 210−221.

(37) Wisen, S., Androsavich, J., Evans, C. G., Chang, L., and Gestwicki, J. E. (2008) Chemical modulators of heat shock protein 70 (Hsp70) by sequential, microwave-accelerated reactions on solid phase. *Bioorg. Med. Chem. Lett. 18*, 60−65.

(38) Wang, A. M., Morishima, Y., Clapp, K. M., Peng, H. M., Pratt, W. B., Gestwicki, J. E., Osawa, Y., and Lieberman, A. P. (2010) Inhibition of Hsp70 by methylene blue affects signaling protein function and ubiquitination and modulates polyglutamine protein degradation. *J. Biol. Chem. 285*, 15714−15723.

(39) Leu, J. I., Pimkina, J., Frank, A., Murphy, M. E., and George, D. L. (2009) A small molecule inhibitor of inducible heat shock protein 70. *Mol. Cell 36*, 15−27.

(40) Cho, H. J., Gee, H. Y., Baek, K. H., Ko, S. K., Park, J. M., Lee, H., Kim, N. D., Lee, M. G., and Shin, I. (2011) A small molecule that binds to an ATPase domain of Hsc70 promotes membrane trafficking of mutant cystic fibrosis transmembrane conductance regulator. *J. Am. Chem. Soc. 133*, 20267−20276.

(41) Walter, G. M., Smith, M. C., Wisen, S., Basrur, V., Elenitoba-Johnson, K. S., Duennwald, M. L., Kumar, A., and Gestwicki, J. E. (2011) Ordered assembly of heat shock proteins, Hsp26, Hsp70, Hsp90, and Hsp104, on expanded polyglutamine fragments revealed by chemical probes. *J. Biol. Chem. 286*, 40486−40493.

(42) Chafekar, S. M., Wisen, S., Thompson, A. D., Echeverria, A., Walter, G. M., Evans, C. G., Makley, L. N., Gestwicki, J. E., and Duennwald, M. L. (2012) Pharmacological tuning of heat shock protein 70 modulates polyglutamine toxicity and aggregation. *ACS Chem. Biol. 7*, 1556−1564.

(43) Kerns, E. H., and Di, L. (2008) *Blood-brain barrier*, Chapter 10, Academic Press, San Diego.

(44) Thompson, A. D., Scaglione, K. M., Prensner, J., Gillies, A. T., Chinnaiyan, A., Paulson, H. L., Jinwal, U. K., Dickey, C. A., and Gestwicki, J. E. (2012) Analysis of the tau-associated proteome reveals that exchange of hsp70 for hsp90 is involved in tau degradation. *ACS Chem. Biol. 7*, 1677−1686.